Available online at www.sciencedirect.com
SCIENCE DIRECT
Polymer 46 (2005) 6016–6024
polymer
www.elsevier.com/locate/polymer

Fracture energy–fracture stress relationship for weak polymer–polymer interfaces

Yuri M. Boiko[a,*], Jørgen Lyngaae-Jørgensen[b]

[a]Fracture Physics Department, A.F. Ioffe Physico-Technical Institute, Politekhnicheskaya 26, St Petersburg 194021, Russian Federation
[b]Danish Polymer Centre, Technical University of Denmark, Building 423, DK-2800 Kongens Lyngby, Denmark

Received 3 March 2005; received in revised form 4 May 2005; accepted 18 May 2005
Available online 15 June 2005

Abstract

The bulk thick films of high-molecular-weight atactic polystyrene (PS) were brought into contact at a small contact pressure ≤ 0.2 MPa at a constant healing temperature T_h below the calorimetric glass transition temperature of the bulk T_g^{bulk}. Fracture energy G and fracture stress σ of the auto-adhesive joints PS–PS were measured at ambient temperature in the T-peel test and the lap-shear joint geometry, respectively. In the framework of the diffusion controlled mechanism of the development of these two mechanical properties suggesting their evolution as $G \propto t_h^{1/2}$ and $\sigma \propto t_h^{1/4}$ (t_h is the healing time), and as $G \propto 1/T_h$ and $\sigma \propto 1/T_h$, a linear relationship between $G^{1/2}$ and σ, valid over a temperature range of $T_h = T_g^{bulk} - 23$ °C to $T_h = T_g^{bulk} - 43$ °C, has been found. The penetration depth of 0.5 nm corresponding to the value of G calculated using the measured value of σ developed at $T_h = T_g^{bulk} - 53$ °C for 24 h was reasonably smaller than the thickness of the surface mobile layer of 1 nm predicted by Wool's rigidity percolation theory for thick bulk PS films. The feasibility of a full healing of polymer–polymer interfaces below T_g^{bulk} has been discussed. The dependence of an apparent activation energy characterising the process of segmental motions at PS surfaces and interfaces on the approach and the physical property chosen for its calculation has been analysed.

Keywords: Polystyrene; Autoadhesion; Fracture properties

1. Introduction

The measurement of the lap-shear strength σ of the contact zone of two flat polymeric surfaces as a function of the contact (or healing) time t_h and temperature T_h can be successfully used for studying the molecular dynamics at polymer–polymer interfaces at fairly low temperatures [1,2]. By the help of this method, the auto-adhesion between two identical thick bulk films of high-molecular-weight (HMW) polymers (having the number-average molecular weight M_n larger than the entanglement molecular weight M_{ent}) was revealed at unexpectedly low T_h in regard to the calorimetric bulk glass transition temperature T_g^{bulk} measured at heating rates of 10–20 °C/min: at $T_h = T_g^{bulk} - 126$ °C, $T_h = T_g^{bulk} - 85$ °C, and $T_h = T_g^{bulk} - 82$ °C for the auto-adhesive joints PPO–PPO [1], PMMA–PMMA [3], and PS–PS [4], respectively [PPO, PMMA, and PS denote, respectively, poly(phenylene oxide), poly(methyl methacrylate), and polystyrene].

The low-temperature auto-adhesion (at $T_h \ll T_g^{bulk}$) [1–4] was explained by the feasibility of the diffusion of chain segments across the viscoelastic contact zone at $T_g^{interface} < T_h < T_g^{bulk}$ ($T_g^{interface}$ is the T_g at the contact zone). This hypothesis has been supported by the observation of interdiffusion across a PS–PS contact zone at T_h approximately equal to $T_g^{bulk} - 20$ °C in recent experiments on neutron reflectivity and dynamic secondary ion mass spectroscopy [5]. Thus, an effect of the lowering of the T_g at the polymer-air or polymer-vacuum interface $T_g^{surface}$ in comparison with T_g^{bulk} prior to contact ($T_g^{surface} < T_g^{bulk}$) [6] persists at a polymer–polymer interface ($T_g^{interface} < T_g^{bulk}$). Actually, the value of $T_g^{interface}$ is hardly expected to heighten significantly towards T_g^{bulk} upon the physical contact of the surfaces at the expense of only van-der-Waals forces of attraction in the absence of mass transfer across the interface [7].

Another important property characterising the adhesion at low T_h is fracture energy G. Indeed, if a G value

* Corresponding author. Tel.: +7 812 2479139; fax: +7 812 2471017.
E-mail address: yuri.boiko@pop.ioffe.rssi.ru (Y.M. Boiko).

0032-3861/$ - see front matter © 2005 Elsevier Ltd. All rights reserved.
doi:10.1016/j.polymer.2005.05.064

developed after the contact of two polymeric surfaces at $T_h \ll T_g^{bulk}$ is larger than the work of adhesion W_a (required to overcome only the forces of physical attraction between the surfaces), it implies the occurrence of mass transfer (segmental diffusion) across the contact zone (if there is no chemical bonding between the groups belonging to the chains located on the opposite sides of the interface and when an undesirable mass transfer due to plastic flow has little chance to occur by the application of a very small pressure to the contact zone.). Therefore, the use of this approach makes it possible to determine the shortest time and the lowest temperature sufficient for the realisation of the translational displacement of chain segments. In this context, an energy term having as a reference W_a seems to be more informative than a strength term.

The applicability of the T-peel test giving an access to G for studying the molecular motions at the contact zone of the thick films of amorphous HMW PS at $T_h < T_g^{bulk}$, down to $T_h = T_g^{bulk} - 43$ °C, has been demonstrated in a recent work [8]. However, very small values of peel force, of order of grams, measured at ambient temperature after bonding the PS–PS auto-adhesive joints at the above conditions, along with the fragility of PS upon bending, turned out to be the drawbacks of this method.

Contrary to the T-peel test, the lap-shear joint method provides markedly larger values of force at break [1–4]. Hence, for studying the healing process leading, at $T_h < T_g^{bulk}$, to the build-up of weak interfaces, it is important to find a correlation between the energy and the strength term in order to convert σ into G when a G value cannot be measured experimentally. For this purpose, the HMW PS–PS auto-adhesive joints were bonded in the T-peel test and the lap-shear joint geometry at $T_h < T_g^{bulk}$ and their fracture energy and fracture stress were measured at $T_h \ll T_g^{bulk}$. A simple empirical relationship between G and σ has been found.

2. Time and temperature dependence of fracture properties

Above T_g^{bulk}, the time and temperature dependencies for the process of the segmental diffusion across the interface of two identical pieces of a polymer have the following forms. According to the crack healing theory [9], the diffusion depth X in the direction normal to the interface plane at t_h shorter than the so-called reptation time is given by Eq. (1).

$$X = a(2Dt_h)^{1/4} \tag{1}$$

where D is the curvilinear diffusion coefficient and a is a constant. This theory as well as the minor chain reptation model [10,11] assume the relationships between the molecular properties (e.g. X) and the fracture properties as $\sigma \propto X$ and $G \propto X^2$. Hence, σ and G may be expressed as

$$\sigma = b(2Dt_h)^{1/4} \tag{2}$$

$$G = c(2Dt_h)^{1/2} \tag{3}$$

where b and c are constants.

The relationship between the fracture energy and the fracture stress is given by this approach as

$$G^{1/2} \propto \sigma \tag{4}$$

The measured values of G and σ will be investigated on their correspondence to Eq. (4) at $T_h < T_g^{bulk}$.

The temperature dependence of D has an Arrhenius form:

$$D = D_0 e^{-E_a/RT} \tag{5}$$

where D_0, E_a, and R are a pressure dependent constant, an apparent activation energy for diffusion, and the universal gas constant, respectively. Replacing D in Eqs. (2) and (3) by its expression from Eq. (5), one obtains

$$\sigma = b' e^{-E_a/4RT} t_h^{1/4} \tag{6}$$

$$G = c' e^{-E_a/2RT} t_h^{1/2} \tag{7}$$

where b' and c' are the proportionality coefficients including $(2D_0)^{1/4}$ and $(2D_0)^{1/2}$, respectively. Taking the logarithm from the two parts of Eqs. (5)–(7), we have, for a constant t_h, Eqs. (8)–(10), respectively.

$$\ln D = \ln D_0 - \frac{E_a}{RT_h} \tag{8}$$

$$\ln \sigma = \ln b'' - \frac{E_a}{4RT_h} \tag{9}$$

$$\ln G = \ln c'' - \frac{E_a}{2RT_h} \tag{10}$$

where b'' and c'' are constants.

As follows from Eqs. (8) to (10), the value of E_a characterising the same diffusion process is directly proportional to $\log D$, $4 \log \sigma$ or $2 \log G$. Thus, the values of E_a calculated from the Arrhenius plots $\ln D - 1/T_h$ $[E_a(D)]$, $\ln G - 1/T_h[E_a(D)]$, and $\ln \sigma - 1/T_h[E_a(\sigma)]$ will be interrelated as:

$$E_a(D) : E_a(G) : E_a(\sigma) = 4 : 2 : 1 \tag{11}$$

This important circumstance should be taken into consideration when comparing the E_a values calculated from the different physical properties measured at polymer–polymer interfaces.

3. Experimental

3.1. Polymer

Commercially available atactic PS with $M_w =$ 225 kg/mol, $M_w/M_n = 3$, $T_g^{bulk} = 97$ °C (the middle point of

the heat capacity jump as measured on a differential scanning calorimeter at a 10 °C/min heating rate) was chosen for this study.

3.2. Preparation of samples

Films of a thickness of 50 (for the T-peel test) or 100 μm (for the lap-shear test) were compression moulded between the smooth surfaces of silicone glass at 165 °C in a Carver press. The film surfaces had a featureless pattern, as observed by scanning electron microscopy, similar to those reported for PS in Ref. [1] (extruded films) and Ref. [3] (the same compression moulding between silicone glass as used here). The films were cut into rectangular strips 5 mm wide.

3.3. Healing procedure

The strips were brought into contact at an area of 5×10 mm^2 (T-peel test) or 5×5 mm^2 (lap-shear test). In order to facilitate good wetting between two surfaces, a small contact pressure of 0.1 (T-peel test) or 0.2 MPa (lap-shear test) was applied to each of the contact zone by a centred dead load. An assembly with 20 coupled strips under loads was placed into preheated oven supplied with a ventilator and controlled at ±1 °C. The healing temperatures were $T_h=44$, 54, 64 and 74 °C. In order to avoid an undesirable fracture of the lap-shear joints bonded at $T_h=74$ °C in the tensile mode, the 250 μm thick strips were used in this case. The longest healing time t_h was 24 h.

3.4. Fracture tests

The bonded PS–PS joints were fractured in the lap-shear and the T-peel geometry on an Instron tester and on a filament stretching rheometer [12], respectively. In all cases, mechanical testing was performed at ambient temperature at a crosshead speed of 5 mm/min. The lap-shear strength σ was calculated as force at break divided by the contact area. The fracture energy G in the T-peel test (peeling at 180°) was calculated as $G=2F_p^{max}/b$, where F_p^{max} and b are the largest peeling force observed for one measurement and the width of the contact zone, respectively. At least 10 joints bonded at the same healing conditions were fractured to measure σ or G. The T-peel test and the lap-shear joint geometry used in this work are shown in Figs. 1 and 2, respectively. More details of the experimental procedures can be found elsewhere [7,8].

4. Results and discussion

4.1. Force at break in the T-peel and lap-shear tests

The shape of the force–displacement curves measured in the lap-shear geometry was similar to those reported previously for the same geometry [1], i.e. a steady increase in force with displacement until the joint fracture has occurred. In Fig. 3, the force–displacement curve recorded upon testing the PS–PS T-peel joint bonded for 24 h at the lowest $T_h=54$ °C used for this geometry is shown. It is seen that the crack propagation results in large fluctuations in the peel force F_p reaching its largest value F_p^{max} upon the joint fracture. This F_p^{max} value is very small being less than a half gram. Beside the curve shown in Fig. 3, for one series of the joints (bonded under the same conditions), peel force may be the largest at small displacements or fluctuate with large amplitude with displacement [8]. All this made it difficult to calculate an average value of F_p for a single measurement as well as for a series. However, the value of F_p^{max} was found to be well reproducible (see the standard deviation of the mean shown by error bars in figures below) and it was chosen for the calculation of G.

In Fig. 4, the value of F_p^{max} measured in the T-peel test geometry is plotted versus the force at break measured in the lap-shear joint geometry F_{l-s}^{b} for PS–PS interfaces.

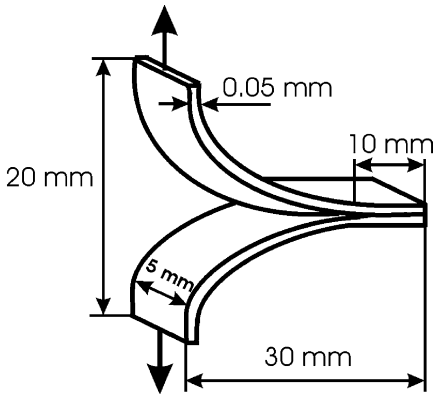

Fig. 1. T-peel test geometry used in this work.

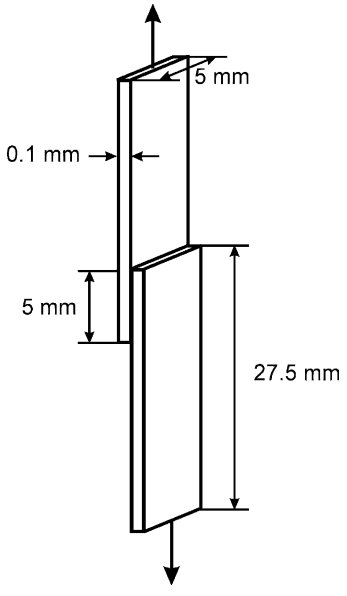

Fig. 2. Lap-shear joint geometry used in this work.

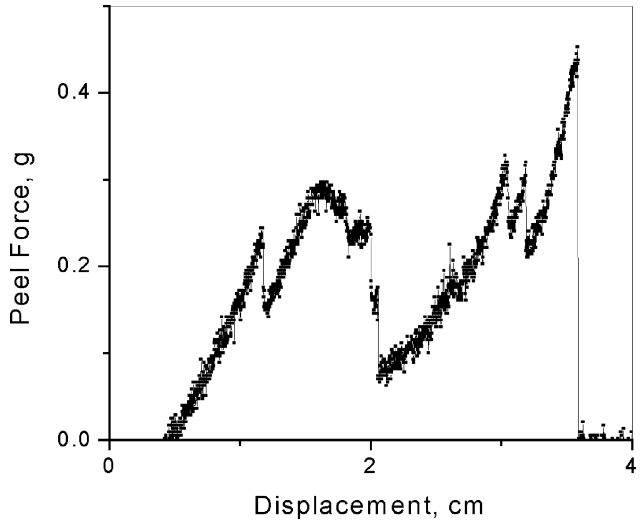

Fig. 3. Peel force as a function of displacement measured at room temperature for a PS–PS interface healed at $T_h = 54$ °C for $t_h = 24$ h.

Each point on this graph corresponds to the same T_h and t_h. As seen, the value of F^b_{l-s} is larger by 2–3 orders of magnitude than the corresponding value of F^{max}_p. This observation may be explained by the simultaneous resistance of the major fraction of the segments, that penetrated across the interface, upon loading the bonded interface in the lap-shear joint geometry, until 'an instantaneous joint fracture', observed in this work, occurred. By contrast, in the T-peel test geometry, the fracture process is localised in the crack tip zone where the interface resistance is provided by the penetrated segments belonging to a very small fraction of the total bonded area. At short t_h and low T_h, there was a problem of the registration of the very small values of $F^b_p < 1$ g since preloading of the bonded area, unavoidable upon fixing the joint in the grips of the tester, may cause the joint fracture prior to testing. Thus, the use of the lap-shear joint geometry allows one to study the molecular mobility and adhesion in polymers at significantly lower temperatures in comparison with those by the use of the T-peel joint geometry.

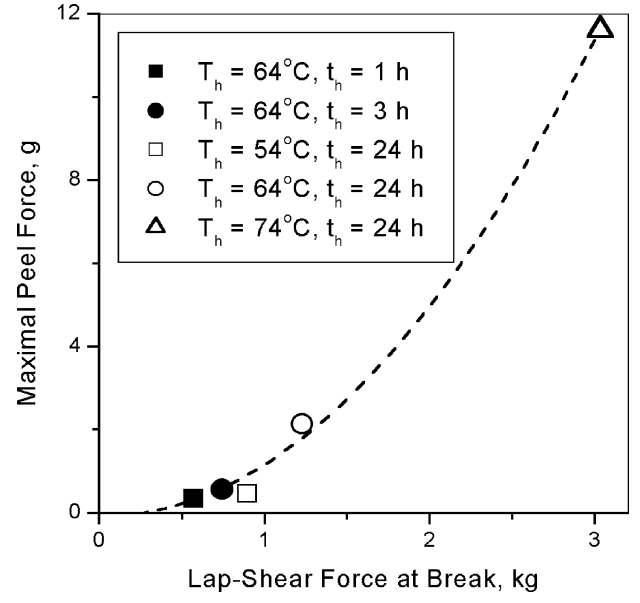

Fig. 4. Maximal peel force as a function of lap-shear force at break for PS–PS interfaces bonded at 54, 64 and 74 °C. A dashed line is drawn as a guide to the eye.

4.2. Time and temperature dependence of fracture energy and fracture stress

In order to investigate the correspondence of the evolution of G and σ at $T_h < T^{bulk}_g$ to the scaling laws predicted by the crack healing theory and the minor chain model [Eqs. (2) and (3)] at $T_h > T^{bulk}_g$, the values of G and σ developed at a PS–PS interface at $T_h = 64$ °C ($= T^{bulk}_g - 33$ °C) are plotted as a function of $t_h^{1/2}$ and $t_h^{1/4}$, respectively, in Fig. 5. As follows from Fig. 5, G and σ increase linearly with $t_h^{1/2}$ (the correlation coefficient k is equal to 0.991) and $t_h^{1/4}$ ($k = 0.992$), respectively. Besides, the smallest value of $G = 1.4$ J/m^2 measured at room temperature after the contact of PS with PS at $T_h = 64$ °C for 1 h is larger by one order of magnitude than the work of adhesion $W_a = 0.084$ J/m^2 for PS at room temperature [13]. Since the creation of the chemical bonds across a PS–PS interface is not feasible, this observation indicates that the contribution of the diffusion of the PS segments into the healing process is larger than the wetting contribution even at $T_h = T^{bulk}_g - 33$ °C and $t_h = 1$ h.

In Fig. 6, the log G and log σ of the PS–PS joints bonded for $t_h = 24$ h are plotted versus $1/T_h$. A linear response corresponding to an Arrhenius behaviour is observed for the two fracture properties. The values of E_a calculated from the slopes to the curves are $E_a(\sigma) = 65$ kJ/mol and $E_a(G) = 151$ kJ/mol. The fact that the value of $E_a(G)$ is twice as large as the value of $E_a(\sigma)$ is in accord with Eq. (11).

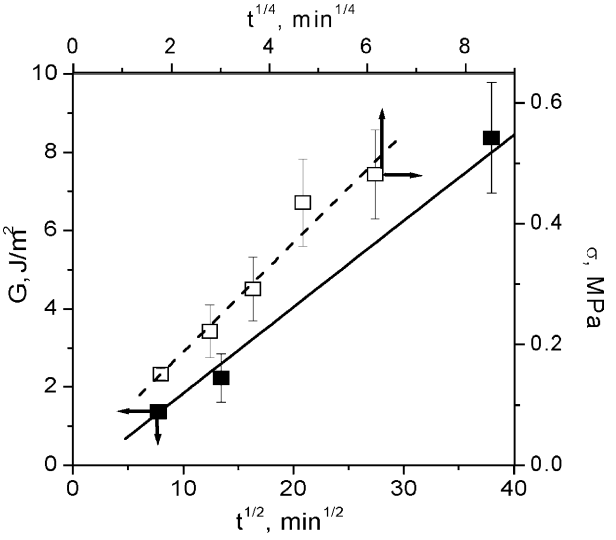

Fig. 5. Fracture energy vs $t_h^{1/2}$ and fracture stress vs $t_h^{1/4}$ measured at room temperature for PS–PS interfaces healed at $T_h = 64$ °C.

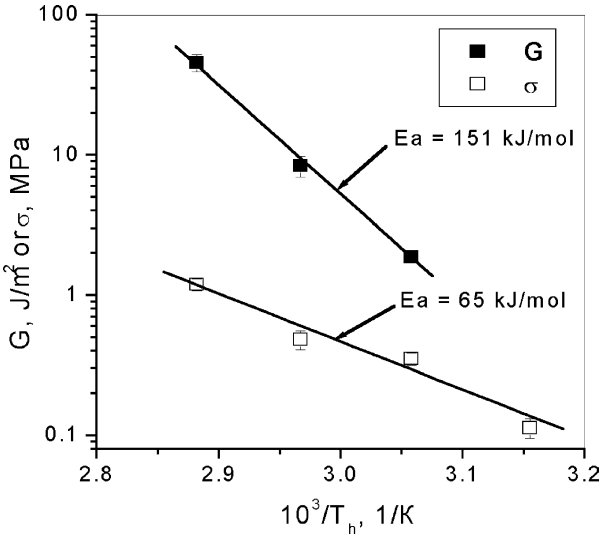

Fig. 6. log G and log σ as a function of $1/T_h$; $t_h = 24$ h.

Thus, both the time and the temperature dependence of G and σ are indicative of the diffusion mechanism of their development at $T_h < T_g^{bulk}$.

4.3. Fracture energy vs fracture stress

In order to investigate the relationship between G and σ in the form of Eq. (4), $G^{1/2}$ is plotted as a function of σ in Fig. 7. Each point reported in Fig. 7 corresponds to the same T_h and t_h for the T-peel test and the lap-shear test geometry. Such plots were constructed for $T_h = 64$ °C (at $t_h = 1$, 3 and 24 h) (inset 'a') and $t_h = 24$ h (for $T_h = 54$, 64 and 74 °C) (inset 'b'). A linear fit of the data presented in the insets 'a' and 'b' of Fig. 7 seems to be satisfactory since it gives a

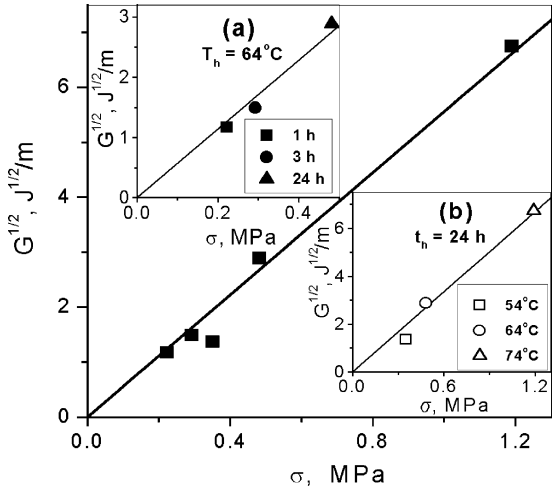

Fig. 7. $G^{1/2}$ vs σ for PS–PS interfaces (each point corresponds to the same T_h and t_h in the T-peel test and the lap-shear joint geometry). Inset (a) $T_h =$ 64 °C; $t_h = 1$ (a solid square), 3 (a solid circle) and 24 h (a solid triangle); inset (b) $t_h = 24$ h; $T_h = 54$ (an open square), 64 (an open circle), and 74 °C (an open triangle). The data from the insets (a) and (b) are plotted as a single graph in the central part (solid squares).

nearly the same slope K to the curves $G^{1/2} = K\sigma$ equal to 5.7 (inset 'a') and 5.6 (inset 'b'). The closeness of the values of K observing for both the time and the temperature dependency of $G^{1/2} = K\sigma$ allows one to consider the two plots from the insets 'a' and 'b' together in the central part of Fig. 7 (solid squares). A linear fit of these data confirms the validity of Eq. (4) with $k = 0.993$:

$$G^{1/2} = 5.6\sigma \tag{12}$$

This correlation between the fracture energy and the fracture stress found for week polymer–polymer interfaces further supports the idea of the feasibility of the diffusion of chain segments across the contact zone well below T_g^{bulk}.

Attempts to measure the value of G in the T-peel test geometry for a PS–PS interface bonded at $T_h < 54$ °C, at $T_h = 44$ °C for $t_h = 24$ h, met with various degrees of success because of very small values of F_p^{max}. However, it was still possible to reliably measure the lap-shear strength of the PS–PS interface ($\sigma = 0.113$ MPa) after its healing under the same conditions. Substituting $\sigma = 0.113$ MPa into Eq. (12), one obtains $G = 0.4$ J/m^2. This value of G is still larger, by a factor of five, than the value of $W_a = 0.084$ J/m^2 for PS. Hence, a period of time of 24 h should be sufficient for the PS segments to diffuse a certain distance across the contact zone PS–PS at a temperature as low as $T_h = T_g^{bulk} - 53$ °C.

Let us now calculate the depth of diffusion X corresponding to the smallest measured ($G = 1.9$ J/m^2) and the calculated with Eq. (12) value of $G = 0.4$ J/m^2 using Eq. (13) [11]:

$$\frac{G}{G_\infty} = \left(\frac{X}{X_\infty}\right)^2 \tag{13}$$

where G_∞ and X_∞ are the fracture energy and the diffusion depth, respectively, for a fully healed interface. With $G_\infty =$ 59 J/m^2 and $X_\infty = 7$ nm calculated for a PS–PS interface with $M_n = 75$ kg/mol [8] (the same PS as used in this work), we have $X = 1.2$ nm (using $G = 1.9$ J/m^2) and $X = 0.55$ nm (using $G = 0.4$ J/m^2), respectively, for $T_h = T_g^{bulk} - 43$ °C and $T_h = T_g^{bulk} - 53$ °C ($t_h = 24$ h in the two cases). This evaluation indicate that, even at $T_h = T_g^{bulk} - 53$ °C, the depth of the diffusion of chain segments across the interface in the direction normal to the interface plane for one day corresponds to the length of the two PS repeat units. For a range of higher T_h, Eq. (13) gives $X = 2.6$ nm ($T_h = T_g^{bulk} - 33$ °C, $t_h = 24$ h) and $X = 5.9$ nm ($T_h = T_g^{bulk} - 23$ °C, $t_h = 24$ h) which compare with the depth of diffusion of 3.5–4 nm across a PS–PS ($M_n = 76$ and 116 kg/mol) contact zone at T_h approximately equal to $T_g^{bulk} - 20$ °C reported by Kajiyama and co-workers [5] (neutron reflectivity and dynamic secondary ion mass spectroscopy measurements).

Very recently, the rigidity percolation theory of thin films melting and the glass transition has been proposed by Wool [14]. For the surface of thick bulk films, this theory defines the depth of the mobile surface layer X_c as

$$X_c = \frac{b(1-p_c)}{(p_c)^{\nu}(1-T/T_g)^{\nu}} \quad (14)$$

where b, p_c, ν, T, and T_g are the bond length, the gradient percolation threshold, the critical exponent for the cluster correlation length, a current temperature (in degrees of Kelvin), and T_g^{bulk}, respectively. Using $b=0.154$ nm, $p_c=0.4$, $\nu=0.82$ [14] at $T_h = T_g^{bulk} - 53$ °C for PS with $T_g^{bulk} = 97$ °C, Eq. (14) gives $X_c=0.96$ nm. This value of X_c is larger, as it should be, than the value of $X=0.55$ nm calculated above with Eq. (13) for the G developed at $T_h = T_g^{bulk} - 53$ °C for 24 h. Thus, there is good agreement between this theory and our approach.

In principle, the latter value of $X=0.55$ nm is small relative to the surface roughness of any macroscopic polymeric sample which, naturally, cannot be 'absolutely flat', since the roughness of the most flat polymer surface should be defined by the size of the Kuhn's segment. For instance, the end-to-end vector of the PS Kuhn's segment consisting of six repeat units equals 1.7 nm. However, if the surface layer is in the viscoelastic state the physical contact at the molecular level between the highest points of the contacting surfaces may be spread over the total interface area fairly rapidly under a slight pressure due to viscoelastic deformation (the case of 'instant wetting' [9]), as it does above T_g^{bulk}. Possibly, after the physical contact is achieved over the total interface area, the interface plane is still not 'completely flat'. But most important is how deep, on the average, can then the segments diffuse across this interface at all contact sites. In other words, the value of X characterises the displacement of the diffusion front.

Our assumption of the rapid wetting seems to be reasonable since we observe the strength growth with $t^{1/4}$, in accordance with the instant wetting approach [9] (wetting occurring very rapidly at the total interface area is followed by diffusion across an interface), and not with $(t+t^{5/4})$ predicted by the constant rate wetting approach [9] (wetted area spreads at a certain rate; simultaneously, diffusion across the wetted areas occurs). Besides, if some fraction of the surface area remained non-wetted, 'the true values' of G, and, therefore, 'the true values' of X, must be larger than those calculated above, i.e. $X>5.9$ nm at $T_h = T_g^{bulk} - 23$ °C and $X>0.55$ nm at $T_h = T_g^{bulk} - 53$ °C. However, neutron reflectivity gives a smaller value of $X=4$ nm at $T_h = T_g^{bulk} - 19$ °C [5] than the former one, and the latter one is reasonably smaller than the depth of the PS mobile layer of 1 nm predicted by the rigid percolation theory at $T_h = T_g^{bulk} - 53$ °C. Thus, both the largest and the smallest value of X calculated from G have the proper reference upper and lower limits and they seem not to be underestimated.

4.4. On the feasibility of full interface healing below T_g^{bulk}

One of the questions of fundamental significance in polymer physics is whether a full interface healing, i.e. the recovering of the interpenetrated structure of the bulk, is feasible below T_g^{bulk}. This issue is still a controversial one. At first sight, even if there is an increased mobility in the surface layer prior to contact the diffusion across an interface might slow down as healing progresses and the entanglement density recovers. Then, the diffusion might arrest if the chain segments reach the immobile bulk layer. In this context, the question regarding the depth of the surface mobile layer X_m^{surf}, in particular, whether this depth is dependent on the size of a macromolecule arises. For example, Kawana and Jones [15] reported a value of X_m^{surf} of 10 nm for the monodisperse PS with both $M_w=275$ and 1950 kg/mol, as measured by ellipsometry over a temperature range of 30–90 °C. This value of X_m^{surf} is smaller than the radius of gyration R_g of an unperturbed chain of 17 nm for the polymer with $M_w=275$ kg/mol. In view of the argument that the full interface healing requires the chain displacement $X^{full}=0.8R_g$ [11], the value of $X_m^{surf}=10$ nm is still smaller than the value of $0.8R_g$ of 13.7 nm for the PS with $M_w=275$ kg/mol. However, as was demonstrated in experiments on dynamic secondary ion mass spectroscopy by Kajiyama and co-workers [5], the depth of diffusion perpendicularly to the PS–PS interface with $M_n=29$ kg/mol attainable at $T_g^{bulk} - 10$ °C and $T_g^{bulk} - 20$ °C is about 5 nm (corresponds to the total interface width of 10 nm), i.e. it is almost the same as R_g of this polymer of ~5 nm. Hence, the PS–PS interface with $M_n=29$ kg/mol investigated in Ref. [5] could be completely healed at a temperature as low as $T_g^{bulk} - 20$ °C.

Let us now evaluate the time to achieve full healing t_h^{full} for the PS–PS interface investigated sufficient for the development of the fracture energy in the virgin state $G_\infty = 59$ J/m^2 for this molecular weight [8]. Extrapolation of the curve $G - t_h^{1/2}$ to $G_\infty = 59$ J/m^2 in Fig. 5 predicts a t_h^{full} value of 49 days at $T_h = T_g^{bulk} - 33$ °C. At a higher $T_h = T_g^{bulk} - 23$ °C, the value of t_h^{full} for this interface is evaluated to be 40 h (using $G=46$ J/m^2 developed for 24 h at this T_h and taking into account that $G \propto t_h^{1/2}$). For the monodisperse PS–PS interface with a larger M_n of 192 kg/mol, $G_\infty = 514$ J/m^2 and the value of G measured in the same T-peel test geometry ($T_h = T_g^{bulk} - 33$ °C, $t_h=24$ h) is 8.4 J/m^2 [8]. Assuming the same rate growth of G for this interface as that observed for the polydisperse PS in Fig. 5, we have $t_h^{full} = 10$ years for the monodisperse PS–PS interface, which is a very long period of time. Nevertheless, a reasonable smaller realistic value of $t_h^{full} = 4$ months is predicted for the monodisperse PS–PS interface when assuming the same ratio of t_h^{full} ($T_h = T_g^{bulk} - 23$ °C):t_h^{full} ($T_h = T_g^{bulk} - 33$ °C) of 1:29.4 which was calculated for the polydisperse PS–PS interface. Thus, this evaluation stimulates further investigations of this phenomenon.

The feasibility of the full healing of polymer–polymer interfaces below T_g^{bulk} is also supported by the molecular dynamics simulation of Mansfield and Theodorou [16] for atactic polypropylene: according to their prediction, the

depth of the surface mobile layer corresponds to $1.3R_g$ at $T_g^{bulk} - 22$ °C.

4.5. Activation energy

In Table 1 are compared the values of $E_a(G)$ and $E_a(\sigma)$ calculated above with the values of E_a for several PSs available in the literature [17–26]. These E_a values were calculated from the mechanical properties (σ, G, lateral force F_{lat}) or from the diffusion coefficient D. For their calculation, three kinds of plots were employed: (i) the Arrhenius plot $\ln(\sigma, G \text{ or } D) - 1/T$, (ii) $\ln a_T(\sigma \text{ or } F_{lat}) - 1/T$ given by the classical principle of time–temperature superposition [Eq. (15)], or (iii) $\ln[\text{slope}(\sigma - t^{1/4} \text{ or } G - t^{1/2})] - 1/T$ [Eq. (16)] based on the reptation mechanism of the evolution of σ or G (see, for instance, Refs. [26,27]).

$$\ln a_T = -\frac{E_a}{R}\left(\frac{1}{T} - \frac{1}{T_0}\right) \tag{15}$$

where $\ln a_T$ is the horizontal shift factor of a physical property along the time or rate axes, T_0 is a reference T_h, and T is a current T_h.

$$E_a = \frac{R \ln\left(\dfrac{\left[(\sigma_2 - \sigma_1)/\left(t_2^{1/4} - t_1^{1/4}\right)\right]_{T1}}{\left[(\sigma_2 - \sigma_1)/\left(t_2^{1/4} - t_1^{1/4}\right)\right]_{T2}}\right)}{(1/T_2) - (1/T_1)} \tag{16}$$

where σ_1 and σ_2 are the values of σ developed for t_1 and t_2 at a constant healing temperature (T_1 or T_2).

As follows from Table 1, the values of $E_a(\sigma) = 65$–69 kJ/mol at $t_h = 24$ h calculated from the plots $\ln \sigma - 1/T$ at $T < T_g^{bulk}$ are independent of M_w and polydispersity ([17,18], this work). These values of $E_a(\sigma)$ are close to the values of

Table 1
Some characteristics and values of an apparent activation energy E_a for several PS–PS interfaces, free PS surfaces or PS films calculated from the mechanical measurements or the diffusion coefficient by the use of different approaches

Sample thickness	$M_w \times 10^{-3}$, g/mol	M_w/M_n	DSC T_g^{bulk}, °C	Temperature range, °C	Measured property	Plot used for calculation of E_a	E_a, kJ/mol	Reference
3.2 mm	262	1.83	100	109–118	σ	$\ln a_T - 1/T$	403	[22]
						$\ln[\text{slope}(\sigma - t^{1/4})] - 1/T$	450[a]	
						$\ln \sigma - 1/T$ ($t_h = 16$ min)	151[a]	
						($t_h = 4.3$ h)	119[a]	
0.1–3 mm	200	1.06	105	90–100	G	$\ln[\text{slope}(G - t^{1/2}) - 1/T$	520	[26]
	225	1.5	96	80–100			210	
0.1 mm	230	2.84	103	55–90	σ	$\ln a_T - 1/T$	415	[17]
						$\ln \sigma - 1/T$ ($t_h = 2$ min)	77[a]	
						($t_h = 24$ h)	65[a]	
0.1 mm	230	2.84	103	62–90	σ	$\ln[\text{slope}(\sigma - t^{1/4}) - 1/4 \ln T] - 1/T$	121	[25]
						$\ln[\text{slope}(\sigma - t^{1/4})] - 1/T$	126[a]	
0.1 mm	1111	1.15	106	53–93	σ	$\ln \sigma - 1/T$ ($t_h = 24$ h)	69	[18]
41–162 mm	1460	1.04	105	66–86	F_{lat}	$\ln a_T - 1/T$	210–240	[23]
200 nm	140	1.06	108	60–110	F_{lat}	$\ln a_T - 1/T$	220	[24]
1 mm	150	1.02	105	125–155	D	$\ln D - 1/T$	201	[20]
	185	1.02	105	125–155			230	
–	2.4	1.1	–	150–179	D	$\ln D - 1/T$	88[a]	[19]
	2.4			179–250			62	
–	9.2	1.1	–	180–208			102[a]	
	9.2			208–250			63	
100–400 nm	111	1.05		128–140	D	$\ln D - 1/T$	356	[21]
	199	1.03		133–147			269	
	693	1.03		145–173			251	
	1082	1.07		150–170			257	
0.05 mm	215	3	97	54–74	G	$\ln G - 1/T$	151	This work
0.1 mm	215	3	97	44–74	σ	$\ln \sigma - 1/T$	65	This work

Values of E_a calculated from the experiments on lateral force microscopy [23,24], secondary ion mass spectroscopy [21], small-angle neutron scattering [20], modified n.m.r. field-gradient technique [19], lap-shear joint method [17,18,25], lap-shear joint and double cantilever beam methods [26].

[a] Values of E_a, calculated from the data presented in the cited references.

$E_a(D)=62$–102 kJ/mol calculated from the plots $\ln D - 1/T$ for the low-molecular-weight PSs at much higher $T > T_g^{bulk}$ [19]. However, according to Eq. (11), the latter ones should be smaller than the former ones by a factor of four. This result may be explained by different diffusion mechanisms for the short non-entangled PS chains with $M_n=2.4$ and 9.2 kg/mol $< M_{ent}$ [19] (Rouse relaxation) and for the long entangled chains in HMW PS [17,18] (reptation). Actually, the values of $E_a(\sigma)=65$–77 kJ/mol calculated with the Arrhenius equation for $T_h < T_g^{bulk}$ are in accord with the values of $E_a(D)=201$–356 kJ/mol for monodisperse HMW PSs, calculated from the $\log D - 1/T$ plots for $T_h > T_g^{bulk}$ [20,21], since, taking into account Eq. (11), $1/4E_a(D)=50$–90 kJ/mol. This indicates that the diffusion mechanism in HMW PS analysed by the Arrhenius approach in terms of the interface strength σ (at $T < T_g^{bulk}$) or of the diffusion coefficient (at $T_h > T_g^{bulk}$) is characterised by nearly the same activation energy.

$E_a(\sigma)$ is weakly dependent on t_h though the tendency of a decrease in $E_a(\sigma)$ with t_h is seen both at $T > T_g^{bulk}$ [20] and $T < T_g^{bulk}$ [17]. At the same time, the values of $E_a(\sigma)=151$ and 119 kJ/mol at $T > T_g^{bulk}$ [22] are twice as large as the values of $E_a(\sigma)=77$ and 65 kJ/mol at $T < T_g^{bulk}$ [17] (calculated from the plots $\log \sigma - 1/T$ in the two cases).

It is important to note that the values of $E_a(\sigma)=403$ [22] and 415 kJ/mol [17] calculated using the shift factor (the logarithm of the division of the two healing times t_1 and t_2 required for the development of the same value of σ at the healing temperatures T_1 and T_2) are larger by a factor of 3–7 than the values of $E_a(\sigma)$ calculated by the Arrhenius equation when the same values of σ are used in the two cases (in the latter case, only for one constant t_h). This considerable difference between the values of $E_a(\sigma)$ for PS–PS interfaces calculated with Eqs. (9) and (15) is due to the use of $\ln(\sigma_1/\sigma_2)$ in the first case and of $\ln a_T [=\ln(t_1/t_2)]$ in the second one since all other parameters in Eqs. (9) and (15) are the same. Actually, on the average, the value of $\log a_T$ varied by 2 with a 10 °C-increment of T_h, between $T_h = T_g^{bulk} - 13$ °C to $T_h = T_g^{bulk} - 48$ °C [17], whereas, considering the values of σ at $t_h=24$ h from Ref. [17] as a $\log \sigma - 1/T_h$ plot, the value of $\log(\sigma_1/\sigma_2)$ varied only by 0.3 at the same increment of T_h (10 °C).

The values of $E_a(\sigma)$ calculated with Eq. (15) are larger by a factor of 2 than the values of $E_a(F_{lat})=210$–240 kJ/mol of α-relaxation [23,24] for the surfaces of the supported thin films of ultra-high-molecular-weight monodisperse PS ($M_n=1460$ kg/mol, $T_g^{bulk}=105$ °C) and HMW PS ($M_n=140$ kg/mol, $T_g^{bulk}=105$ °C) which were calculated by the same approach (from $\ln a_T - 1/T_h$ plots). Master curves for F_{lat} were constructed over a temperature range of 66–86 °C [23] or of 60–110 °C [24], i.e. always below T_g^{bulk}. This indicates that the process of α-relaxation (disordered micro-Brownian segmental motions) on the free surface above $T_g^{surface}$ is easier realisable (has a smaller activation barrier) than the one-dimensional diffusion of segments across the polymer–polymer interface above $T_g^{interface}$.

Although the calculation of E_a using the $\ln[\text{slope}(\sigma - t_h^{1/4})] - 1/T$ [Eq. (16)] or $\ln a_T - 1/T$ [Eq. (15)] plots considers the process of interface healing as a temperature-activated process developing with time, the use of Eq. (16) might give whether a close result in comparison with that obtained with Eq. (15) ($E_a=450$ and 403 kJ/mol, respectively [22]), or a smaller value of E_a (121–126 [23] and 415 kJ/mol [17], respectively) for the same PS–PS interfaces.

The values of $E_a(G)=210$ and 520 kJ/mol [26] calculated from the plots $\ln[\text{slope}(G - t_h^{1/2})] - 1/T$ with Eq. (16) (replacing σ by G and $t^{1/4}$ by $t^{1/2}$) measured in the lap-shear joint or the double beam cantilever geometry are larger than the value of $E_a(G)=151$ kJ/mol calculated in this work from the Arrhenius plot $\log G - 1/T$. This behaviour is in accord with that one considered above [an E_a value calculated with Eqs. (9) or (10) is always smaller than an E_a value calculated with Eqs. (15) or (16)].

Thus, the E_a value for one and the same PS is strongly dependent on the approach used for its calculation (e.g. the Arrhenius method or the principle of time–temperature equivalence). By contrast, the value of E_a is weakly dependent on the PS molecular weight at $M_n > M_{ent}$ [see, e.g. the $E_a(F_{lat})$ values from Refs. [23,24] or $E_a(\sigma)$ values from Refs. [17,18] and this work] or a property chosen for its calculation (σ, G or D) if a proper exponent multiplier is taken into account [Eq. (11)]. The fact that the values of E_a calculated for both $T > T_g^{bulk}$ and $T < T_g^{bulk}$ might be close is suggestive of the involvement into the diffusion process occurring at $T > T_g^{interface}$ of the 'kinetic units' (segments) of a comparable length in the two cases. Finally, the variation in the sample thickness by 3–5 orders of magnitude has a minor effect on the E_a value. This behaviour reasonably agrees with an importance in all the cases considered of only the thickness of a comparably thin 'activated interface layer' wherein the segmental diffusion proceeds (presumably, nanometers-tens of nanometer).

The physical meaning of the E_a characterising the diffusion process is the energy required to overcome the potential barrier for the realisation of the translational displacement of the chain segments across the interface. From the different approaches used for the calculation of E_a, the use of Eqs. (15) and (16) seems to more correctly characterise the interface healing process since the use of $\ln a_T$ and $\log[\text{slope}(G - t_h^{1/2})]$ or $\log[\text{slope}(\sigma - t_h^{1/2})]$ takes into account not only the temperature, as in the case of the employment of the Arrhenius plots, but the time contribution as well.

5. Conclusions

The complimentary use of the T-peel and the lap-shear joint method has shown to be a useful approach for studying the molecular dynamics in the viscoelastic interface layer of the contacting glassy thick bulk films of PS well below

T_g^{bulk}. The simple empirical relationship between the fracture energy and the fracture stress, $G^{1/2}=K\sigma$, found for the weak PS–PS interfaces gives the possibility to calculate the value of G which could develop at $T_h \ll T_g^{bulk}$ using the measured value of σ developed after the bonding at the same conditions. The calculated value of G which could develop at the PS–PS interface at $T_h = T_g^{bulk} - 53$ °C for 24 h corresponds to the penetration depth of the order of 0.5–0.6 nm. This depth is within the thickness of the surface mobile layer of 1 nm predicted by Wool's rigidity percolation theory for thick bulk PS films at that temperature. The calculated times to achieve the full healing of the HMW PS–PS interfaces at $T_h = T_g^{bulk} - 33$ °C and $T_h = T_g^{bulk} - 23$ °C of the order of weeks-months leave the question of the feasibility of the full interface healing at a certain distance below T_g^{bulk} open, stimulating further study of this phenomenon. The comparison of the apparent activation energies characterising the segmental motions at PS surfaces and interfaces derived from different measurements showed that the E_a value for one and the same PS was strongly dependent on the approach used for its calculation and the chosen physical property.

Acknowledgements

The authors thank Dr A. Bach for recording the peel force-displacement curves and Prof R. P. Wool for bringing his new theory to their attention. Financial support of the Danish Technical Research Council of the Danish Research Agency, including a NATO Senior Science Fellowship granted to Y.M. Boiko, is acknowledged.

References

[1] Boiko YM, Prud'homme RE. Macromolecules 1997;30(12):3708–10.
[2] Boiko YM, Prud'homme RE. Macromolecules 1998;31(19):6620–6.
[3] Boiko YM, Lyngaae-Jørgensen J. Polym Sci 2005;B47(5–6):151–4.
[4] Boiko YM, Lyngaae-Jørgensen J. J Macromol Sci Phys 2004;B43(5):925–34.
[5] Kawaguchi D, Tanaka K, Kajiyama T, Takahara A, Tasaka S. Macromolecules 2003;36(4):1235–40.
[6] Kajiyama T, Tanaka K, Takahara A. Macromolecules 1995;28(9):3482–4.
[7] Boiko YM, Lyngaae-Jørgensen J. Polymer 2004;45(25):8541–9.
[8] Boiko YM, Bach A, Lyngaae-Jørgensen J. J Polym Sci, Part B: Polym Phys 2004;42(10):1861–7.
[9] Wool RP, O'Connor KM. J Appl Phys 1981;52(10):5953–63.
[10] Kim YH, Wool RP. Macromolecules 1983;16(7):1115–20.
[11] Wool RP. Polymer interfaces: structure and strength. Munich: Hanser Press; 1995.
[12] Bach A, Almdal K, Rasmussen HK, Hassager O. Macromolecules 2003;36(14):5174–9.
[13] van Krevelen DW. Properties of polymers. 3rd ed. Amsterdam: Elsevier; 1997.
[14] Wool RP, Sun S. Bio-based polymers and composites. Burlington MA: Elsevier; 2005 [chapter 6].
[15] Kawana S, Jones RAL. Phys Rev E 2001;63:021501/1–021501/6.
[16] Mansfield KF, Theodorou DN. Macromolecules 1991;24(23):6283–94.
[17] Boiko YM, Prud'homme RE. J Appl Polym Sci 1999;74(4):825–30.
[18] Boiko YM. Unpublished results.
[19] Bachus R, Kimmich R. Polymer 1983;24(8):964–70.
[20] Kim DK, Sperling LH, Klein A, Hammouda B. Macromolecules 1994;27(23):6841–50.
[21] Whitlow SJ, Wool RP. Macromolecules 1991;24(22):5926–38.
[22] Kline DB, Wool RP. Polym Eng Sci 1988;28(1):52–7.
[23] Akabori K, Tanaka K, Kajiyama T, Takahara A. Macromolecules 2003;36(13):4937–43.
[24] Kawaguchi D, Tanaka K, Kajiyama T, Takahara A, Tasaka S. Macromolecules 1998;31(15):5150–1.
[25] Boiko YM. Polym Sci 2002;A44(7):723–8.
[26] Guérin G, Mauger F, Prud'homme RE. Polymer 2003;44(24):7477–84.
[27] Cho B-R, Kardos JL. J Appl Polym Sci 1995;56:1435–54.